Cite as: C. Yamashiro *et al.*, *Science* 10.1126/science.aat1674 (2018).

Generation of human oogonia from induced pluripotent stem cells in vitro

Chika Yamashiro[1,2], Kotaro Sasaki[1,2], Yukihiro Yabuta[1,2], Yoji Kojima[1,2,3,4], Tomonori Nakamura[1,2], Ikuhiro Okamoto[1,2], Shihori Yokobayashi[1,2,4], Yusuke Murase[1,2], Yukiko Ishikura[1,2], Kenjiro Shirane[5,6], Hiroyuki Sasaki[5,6], Takuya Yamamoto[3,4,7], Mitinori Saitou[1,2,3,4]*

[1]Department of Anatomy and Cell Biology, Graduate School of Medicine, Kyoto University, Yoshida-Konoe-cho, Sakyo-ku, Kyoto 606-8501, Japan. [2]JST, ERATO, Yoshida-Konoe-cho, Sakyo-ku, Kyoto 606-8501, Japan. [3]Institute for Integrated Cell-Material Sciences, Kyoto University, Yoshida-Ushinomiya-cho, Sakyo-ku, Kyoto 606-8501, Japan. [4]Center for iPS Cell Research and Application, Kyoto University, 53 Kawahara-cho, Shogoin, Sakyo-ku, Kyoto 606-8507, Japan. [5]Division of Epigenomics, Medical Institute of Bioregulation, and Epigenome Network Research Center, Kyushu University, Maidashi 3-1-1, Higashi-ku, Fukuoka 812-8582, Japan. [6]Graduate School of Medical Sciences, Kyushu University, Maidashi 3-1-1, Higashi-ku, Fukuoka 812-8582, Japan. [7]AMED-CREST, AMED, 1-7-1 Otemachi, Chiyoda-ku, Tokyo, 100-0004, Japan.

***Corresponding author. Email: saitou@anat2.med.kyoto-u.ac.jp**

Human in vitro gametogenesis may transform reproductive medicine. Human pluripotent stem cells (hPSCs) have been induced into primordial germ cell-like cells (hPGCLCs); however, further differentiation to a mature germ cell has not been achieved. Here, we show that hPGCLCs differentiate progressively into oogonia-like cells during a long-term in vitro culture (~four months) in xenogeneic reconstituted ovaries with mouse embryonic ovarian somatic cells. The hPGCLC-derived oogonia display hallmarks of epigenetic reprogramming, i.e., genome-wide DNA demethylation, imprint erasure, and extinguishment of aberrant DNA methylation in hPSCs, and acquire an immediate precursory state for meiotic recombination. Furthermore, the inactive X chromosome shows a progressive demethylation and reactivation, albeit partially. These findings establish the germline competence of hPSCs and provide a critical step toward human in vitro gametogenesis.

The germ-cell lineage arises from primordial germ cells (PGCs) that go through a multi-step process to generate spermatozoa or oocytes. Methods for in vitro gametogenesis from pluripotent stem cells (PSCs) would provide a powerful tool to explore the mechanism of germ-cell development and its anomalies (*1*). Mouse PSCs have been induced into PGC-like cells (mPGCLCs), which contribute to spermatogenesis upon transplantation into testes (*2*, *3*) and to oogenesis upon aggregation with embryonic ovarian somatic cells (reconstituted ovaries) followed by transplantation under ovarian bursa (*4*) or an appropriate culture (*5*). Resultant gametes from these procedures generate fertile offspring (*2*–*5*). Furthermore, human PSCs (hPSCs) have been induced into hPGCLCs bearing a gene-expression property of hPGCs just after their specification, opening the possibility for human in vitro gametogenesis (*6*, *7*). However, further differentiation of hPGCLCs has not been successful, and whether hPGCLCs can develop as mature germ cells remains unknown.

At week 2 (Wk2) of development, hPGCs express key transcription factors (TFs) such as SOX17, TFAP2C, and BLIMP1 (also known as PRDM1). Then at Wk5 they migrate to and colonize the embryonic gonads to initiate differentiation into oogonia or gonocytes in embryonic ovaries or testes (*8*, *9*) that express RNA regulators such as DAZL and DDX4 (also known as human VASA homolog: hVH) (*10*–*12*). Oogonia and gonocytes are very similar in morphology, gene expression, and epigenetic properties until they start sexual differentiation at Wk10 into oocytes via meiotic prophase or fetal spermatogonia (*8*–*12*). A characteristic event in germ-cell development is epigenetic reprogramming, which occurs by Wk10 and leads to genome-wide DNA demethylation, imprint erasure, and X reactivation (*10*–*12*).

We explored whether hPGCLCs can undergo further development in vitro in xenogeneic reconstituted ovaries (xrOvaries) with mouse embryonic ovarian somatic cells (Fig. S1A). First, we induced male human induced PSCs (hiPSCs) with the *BLIMP1-tdTomato*; *TFAP2C-EGFP* alleles [585B1 BTAG (XY)] into incipient mesoderm-like cells (iMeLCs) and then into hPGCLCs (*7*, *13*). BLIMP1 and TFAP2C are expressed in oogonia/gonocytes at least until Wk10 (*10*–*12*). We isolated BTAG-positive (BT^+AG^+) hPGCLCs at day 6 (d6) of induction by fluorescence activated cell sorting (FACS), and generated xrOvaries. In agreement with a previous report (*5*), mPGCLCs differentiated efficiently into primary oocytes and formed secondary follicles after a 21-day culture in rOvaries (Fig. S1B). At culture day 7 (ag7), the xrOvaries exhibited a round and flattened shape, and the BT^+AG^+ cells were distributed uniformly within the xrOvaries (Fig. S1C). Subsequently, the xrOvaries expanded laterally with the formation of cyst-like structures (Fig. 1A). From ag21 to ag77, the xrOvaries exhibited auto-fluorescence under fluorescence microscopy (Fig. S1D). There were about 2000 BT^+AG^+ cells per xrOvary at ag21

and ~500 at ag77 (Fig. S1E), indicating that only a fraction of the initial hPGCLCs (~5,000) survived in xrOvaries.

At ag77, the AG$^+$ cells in xrOvaries existed as clusters, were positive for a human mitochondrial antigen, bore faint DAPI staining, and were delineated by FOXL2$^+$ mouse granulosa cells and their basement membrane (Fig. S2A-C). The intensity of the DAPI staining in AG$^+$ cells appeared to decline progressively during the culture (Fig. S2D). The AG$^+$ cells expressed key TFs for early germ cells (TFAP2C, SOX17, POU5F1), and some were mitotically active (Ki67$^+$) or in apoptosis (cleaved CASPASE3$^+$) (Fig. S2A). Importantly, at ag77, many AG$^+$ cells up-regulated DAZL and DDX4 (Fig. 1B, Fig. S2E), suggesting that in xrOvaries, hPGCLCs not only survive as germ cells, but also differentiate into oogonia/gonocytes. Accordingly, at ag77, electron microscopy revealed the presence of large cells, highly similar to oogonia/gonocytes, with clear cytoplasms with sparsely located mitochondria and with round nuclei with loosely packed chromatin and prominent nucleoli (Fig. S3) (*8*, *9*).

We next generated female hiPSCs bearing the AG; *DDX4/hVH-tdTomato* alleles [1390G3 AGVT (XX)] (Fig. S4) (*13*), created xrOvaries, and cultured them up to ag120. The female AG$^+$ hPGCLCs in xrOvaries developed similarly to the male hPGCLCs (Fig. S5), and up-regulated VT at ag77 and the AG$^+$VT$^+$ cells appeared to differentiate into AG-negative (AG$^-$) VT$^+$ cells at ag120 (Fig. 1C, S5A). We examined the expression of key genes by quantitative (q)-PCR. Both male and female hPGCLC-derived cells expressed early germ-cell genes (*BLIMP1*, *TFAP2C*, *SOX17*, *NANOS3*), core/naïve pluripotency genes (*POU5F1*, *NANOG*, *TCL1B*, *TFCP2L1*), and up-regulated genes for oogonia/gonocytes (*DAZL*, *DDX4*) from around ag35/49 onwards, and also genes for meiosis (*SYCP3*, *REC8*) (Fig. S6). The AG$^-$VT$^+$ cells at ag120 down-regulated early germ-cell and core/naïve pluripotency genes, and up-regulated *STRA8*, a gene essential for meiosis initiation (Fig. S6), suggesting their developmentally advanced character. Consistently, the DDX4$^+$ cells at ag120 expressed SYCP3, but not γH2AX, DMC1 and SYCP1 proteins, indicating that they have not yet initiated meiotic recombination (Fig. S7).

We analyzed the transcriptomes of these cell types (Fig. S8A, Table S1). Unsupervised hierarchical clustering (UHC) showed that hPGCLC-derived cells are distinct from hiPSCs/iMeLCs, and can be sub-classified according to their culture period (Fig. S8B). Principle component analysis (PCA) gave a concordant result (Fig. S8C). We identified the genes with significantly positive or negative PC1/2 loadings (453 genes) (Fig. S8D, Table S2). UHC classified them into five major clusters (Fig. 2A, S8D, Table S2): Cluster 1 represents the genes up-regulated upon hPGCLC specification or early in xrOvaries and expressed essentially continuously thereafter. Clusters 2 and 5 signify the genes transiently expressed in early hPGCLC-derived cells or down-regulated early in xrOvaries, and cluster 4 represents the genes down-regulated upon hPGCLC specification (Fig. 2A, Table S2). Cluster 3, which shows a progressive and coordinated up-regulation from ag35 onwards, signifies genes for oogonia/gonocytes and is enriched in genes with gene ontology (GO) functional terms for male meiosis, fertilization, and piRNA metabolic process (Fig. 2A, Table S2). Using the 453 genes, we compared the gene-expression properties of hPGCLC-derived cells with those of oogonia/gonocytes (*12*). hPGCLC-derived cells from ag35 onward, particularly the ag77 BT$^+$AG$^+$/ag120 AG$^+$ cells, exhibited a strong similarity to Wk7/9 oogonia/gonocytes (Fig. 2B, Fig. S10).

The ag120 AG$^-$VT$^+$ cells exhibited a developmentally advanced character (Fig. S6, S7, S8B, C). To clarify this point further, we examined the expression of genes that distinguish relevant human fetal germ cells [FGCs: mitotic (oogonia/gonocytes), retinoic acid (RA)-responsive (female), meiotic (female), oogenesis (female)] (*14*) in ag120 AG$^-$VT$^+$ cells, which, intriguingly, revealed their similarity to RA-responsive FGCs. They down-regulate genes for early germ cells, further up-regulate *DAZL*, *DDX4*, *MAEL* and *KRBOX1*, up-regulate RA- or bone morphogenetic protein (BMP)-responsive genes (*STRA8*, *REC8*, or *ID1/2/3/4*, *MSX1/2*), yet do not sufficiently up-regulate key meiosis genes (*SYCP1*, *DMC1*, *SPO11*, *PRDM9*) (Fig. 2C, S11). Thus, hPGCLC development in xrOvaries reconstitutes human germ-cell development, albeit with protracted kinetics, leading to the generation of oogonia and RA-responsive FGCs, a state responding to the signal for the meiotic entry and in preparation for the meiotic recombination (*14*).

We determined the genome-wide DNA methylation (5-methylcytosine: 5mC) profiles of hPGCLC-derived cells in xrOvaries by whole-genome bisulfite sequencing (WGBS) (Fig. S12A, Table S3). The genome-wide 5mC levels of hiPSCs/iMeLCs were both ~80%, and they decreased progressively in hPGCLC-derived cells, reaching ~20% in ag77 cells and ~13% in ag120 cells (Fig. S12B), the levels comparable to that in oogonia/gonocytes at Wk7/10 (*11*, *12*). The demethylation occurred throughout the genome (Fig. 3, Fig. S12C, S13A, B), and the 5mC distribution profiles of the ag77/ag120 cells were very similar to those of oogonia/gonocytes at Wk7/Wk10 (Fig. 3), respectively, but not to those of the blastocysts (*15*) and naïve hESCs (*16*, *17*) [and hPGCLCs reported by others (*18*)] (Fig. S12D). Thus, hPGCLC-derived cells demethylate their 5mCs in a fashion similar to oogonia/gonocytes, but not early embryonic cells and their putative in vitro counterparts.

We examined whether hPGCLC-derived cells can erase the parental imprints. Blastocysts (*15*) and somatic cells (*11*) exhibited ~50% CpG methylation in the differentially methylated regions (DMRs) of paternally and maternally imprinted genes (Fig. 4A, Table S4). In contrast, hiPSCs and primed hESCs (*12*, *16*, *17*) exhibited hyper-methylation in some DMRs,

whereas naïve hESCs (*16*, *17*) showed hypo-methylation in nearly all the DMRs (Fig. 4A), indicating that hPSCs mis-regulate the imprint states. Similar to oogonia/gonocytes, hPGCLC-derived cells progressively erased the parental imprints, including the hyper-methylated DMRs of hiPSCs (Fig. 4A). We determined the CpG sequences bearing a hypermethylation in hiPSCs compared to three independent hESC lines (Table S5). hPGCLC-derived cells erased such hiPSC-specific methylation in a nearly complete fashion (Fig. S13C). Repeat elements are also demethylated in hPGCLC-derived cells, and the demethylation-resistant repeats in vivo, such as ERVK and SVA (*11*, *12*), showed similar resistance in hPGCLC-derived cells (Fig. S13D). We defined the "escapees" that retained relatively high 5mC levels in ag77/ag120 cells and the Wk7 oogonia/gonocytes (Table S6). Essentially all the escapees in the oogonia/gonocytes (*12*) were included in those in the hPGCLC-derived cells, which were enriched around SVA, ERVK, and ERV1 (Fig. S13E).

We explored whether hPGCLC-derived cells can reactivate the inactive X chromosome (Xi). RNA fluorescence in situ hybridization (RNA FISH) revealed that the 1390G3 AGVT hiPSCs (passage 29) lack the expression of *XIST* from both alleles and show mono-allelic expression of the X-linked genes (Fig. S14A-D), indicating that they bear one active X chromosome (Xa) and one Xi without *XIST* (Xi^{XIST-}) (*19*). Accordingly, the promoters of the X-linked genes in 1390G3 AGVT hiPSCs exhibited an intermediate (~50%) 5mC level (Fig. 4B, S14E, S15), suggesting that they are unmethylated on the Xa and nearly fully methylated on the Xi (*19*). Notably, the ag120 cells, but not d6 hPGCLCs, exhibited a partial (~20%) reactivation, i.e., bi-allelic expression, of several X-linked genes, but did not reactivate *XIST* (Fig. S14A-D). Consistently, the promoters of the X-linked genes in ag120 cells were moderately demethylated (~20%) (Fig. 4B, S14E, S15). These findings demonstrate that hPGCLC-derived cells in xrOvaries undergo proper epigenetic reprogramming, i.e., genome-wide DNA demethylation, imprint erasure, and extinguishment of aberrantly acquired/persisting methylation of hiPSCs, reaching minimum 5mC levels (~13%) comparable to those reported in human germ cells. Nonetheless, the Xi^{XIST-} state in vitro is more resistant to reprogramming, indicating a distinctive epigenetic mechanism for the Xi in hPSCs, which warrants further investigation.

We have provided evidence that primed hiPSCs (*20*) are competent to generate germ cells with their hallmark of epigenetic reprogramming. In mouse-mouse rOvaries, ovarian somatic cells, likely granulosa cells, provide timely signals/environments for mPGCLCs to mature into primary oocytes and form secondary follicles (*5*). In contrast, in xrOvaries, mouse granulosa cells create a permissive environment for hPGCLCs to gradually mature into oogonia. Although the underlying mechanism remains unclear, since mPGCLCs undergo epigenetic reprogramming upon expansion and differentiate into oocytes in response to BMP and RA (*21*, *22*), hPGCLC-derived cell proliferation and signals from mouse granulosa cells (Fig. S16) would allow hPGCLC-derived cells to mature into oogonia/RA-responsive FGCs (Fig. S17). Since both male and female mPGCLCs enter into meiotic prophase under the same condition (*22*), male hPGCLCs would also enter into meiotic prophase in xrOvaries. Future studies will include exploring a strategy and the mechanism for the differentiation of hiPSC-induced oogonia into oocytes with meiotic recombination or for the differentiation of hPGCLCs into fetal spermatogonia, which promote human in vitro gametogenesis.

REFERENCES AND NOTES

1. M. Saitou, H. Miyauchi, Gametogenesis from Pluripotent Stem Cells. *Cell Stem Cell* **18**, 721–735 (2016). doi:10.1016/j.stem.2016.05.001 Medline
2. K. Hayashi, H. Ohta, K. Kurimoto, S. Aramaki, M. Saitou, Reconstitution of the mouse germ cell specification pathway in culture by pluripotent stem cells. *Cell* **146**, 519–532 (2011). doi:10.1016/j.cell.2011.06.052 Medline
3. Y. Ishikura, Y. Yabuta, H. Ohta, K. Hayashi, T. Nakamura, I. Okamoto, T. Yamamoto, K. Kurimoto, K. Shirane, H. Sasaki, M. Saitou, In Vitro Derivation and Propagation of Spermatogonial Stem Cell Activity from Mouse Pluripotent Stem Cells. *Cell Reports* **17**, 2789–2804 (2016). doi:10.1016/j.celrep.2016.11.026 Medline
4. K. Hayashi, S. Ogushi, K. Kurimoto, S. Shimamoto, H. Ohta, M. Saitou, Offspring from oocytes derived from in vitro primordial germ cell-like cells in mice. *Science* **338**, 971–975 (2012). doi:10.1126/science.1226889 Medline
5. O. Hikabe, N. Hamazaki, G. Nagamatsu, Y. Obata, Y. Hirao, N. Hamada, S. Shimamoto, T. Imamura, K. Nakashima, M. Saitou, K. Hayashi, Reconstitution in vitro of the entire cycle of the mouse female germ line. *Nature* **539**, 299–303 (2016). doi:10.1038/nature20104 Medline
6. N. Irie, L. Weinberger, W. W. C. Tang, T. Kobayashi, S. Viukov, Y. S. Manor, S. Dietmann, J. H. Hanna, M. A. Surani, SOX17 is a critical specifier of human primordial germ cell fate. *Cell* **160**, 253–268 (2015). doi:10.1016/j.cell.2014.12.013 Medline
7. K. Sasaki, S. Yokobayashi, T. Nakamura, I. Okamoto, Y. Yabuta, K. Kurimoto, H. Ohta, Y. Moritoki, C. Iwatani, H. Tsuchiya, S. Nakamura, K. Sekiguchi, T. Sakuma, T. Yamamoto, T. Mori, K. Woltjen, M. Nakagawa, T. Yamamoto, K. Takahashi, S. Yamanaka, M. Saitou, Robust In Vitro Induction of Human Germ Cell Fate from Pluripotent Stem Cells. *Cell Stem Cell* **17**, 178–194 (2015). doi:10.1016/j.stem.2015.06.014 Medline
8. T. G. Baker, A Quantitative and Cytological Study of Germ Cells in Human Ovaries. *Proc. R. Soc. London B Biol. Sci.* **158**, 417–433 (1963). doi:10.1098/rspb.1963.0055 Medline
9. T. Fukuda, C. Hedinger, P. Groscurth, Ultrastructure of developing germ cells in the fetal human testis. *Cell Tissue Res.* **161**, 55–70 (1975). doi:10.1007/BF00222114 Medline
10. S. Gkountela, K. X. Zhang, T. A. Shafiq, W.-W. Liao, J. Hargan-Calvopiña, P.-Y. Chen, A. T. Clark, DNA Demethylation Dynamics in the Human Prenatal Germline. *Cell* **161**, 1425–1436 (2015). doi:10.1016/j.cell.2015.05.012 Medline
11. F. Guo, L. Yan, H. Guo, L. Li, B. Hu, Y. Zhao, J. Yong, Y. Hu, X. Wang, Y. Wei, W. Wang, R. Li, J. Yan, X. Zhi, Y. Zhang, H. Jin, W. Zhang, Y. Hou, P. Zhu, J. Li, L. Zhang, S. Liu, Y. Ren, X. Zhu, L. Wen, Y. Q. Gao, F. Tang, J. Qiao, The Transcriptome and DNA Methylome Landscapes of Human Primordial Germ Cells. *Cell* **161**, 1437–1452 (2015). doi:10.1016/j.cell.2015.05.015 Medline
12. W. W. Tang, S. Dietmann, N. Irie, H. G. Leitch, V. I. Floros, C. R. Bradshaw, J. A. Hackett, P. F. Chinnery, M. A. Surani, A Unique Gene Regulatory Network Resets the Human Germline Epigenome for Development. *Cell* **161**, 1453–1467 (2015). doi:10.1016/j.cell.2015.04.053 Medline
13. S. Yokobayashi, K. Okita, M. Nakagawa, T. Nakamura, Y. Yabuta, T. Yamamoto, M. Saitou, Clonal variation of human induced pluripotent stem cells for induction into

the germ cell fate. *Biol. Reprod.* **96**, 1154–1166 (2017). doi:10.1093/biolre/iox038 Medline
14. L. Li, J. Dong, L. Yan, J. Yong, X. Liu, Y. Hu, X. Fan, X. Wu, H. Guo, X. Wang, X. Zhu, R. Li, J. Yan, Y. Wei, Y. Zhao, W. Wang, Y. Ren, P. Yuan, Z. Yan, B. Hu, F. Guo, L. Wen, F. Tang, J. Qiao, Single-cell RNA-seq analysis maps development of human germline cells and gonadal niche interactions. *Cell Stem Cell* **20**, 858–873.e4 (2017). doi:10.1016/j.stem.2017.03.007 Medline
15. H. Okae, H. Chiba, H. Hiura, H. Hamada, A. Sato, T. Utsunomiya, H. Kikuchi, H. Yoshida, A. Tanaka, M. Suyama, T. Arima, Genome-wide analysis of DNA methylation dynamics during early human development. *PLOS Genet.* **10**, e1004868 (2014). doi:10.1371/journal.pgen.1004868 Medline
16. Y. Takashima, G. Guo, R. Loos, J. Nichols, G. Ficz, F. Krueger, D. Oxley, F. Santos, J. Clarke, W. Mansfield, W. Reik, P. Bertone, A. Smith, Resetting transcription factor control circuitry toward ground-state pluripotency in human. *Cell* **158**, 1254–1269 (2014). doi:10.1016/j.cell.2014.08.029 Medline
17. W. A. Pastor, D. Chen, W. Liu, R. Kim, A. Sahakyan, A. Lukianchikov, K. Plath, S. E. Jacobsen, A. T. Clark, Naive Human Pluripotent Cells Feature a Methylation Landscape Devoid of Blastocyst or Germline Memory. *Cell Stem Cell* **18**, 323–329 (2016). doi:10.1016/j.stem.2016.01.019 Medline
18. F. von Meyenn, R. V. Berrens, S. Andrews, F. Santos, A. J. Collier, F. Krueger, R. Osorno, W. Dean, P. J. Rugg-Gunn, W. Reik, Comparative Principles of DNA Methylation Reprogramming during Human and Mouse In Vitro Primordial Germ Cell Specification. *Dev. Cell* **39**, 104–115 (2016). doi:10.1016/j.devcel.2016.09.015 Medline
19. S. Patel, G. Bonora, A. Sahakyan, R. Kim, C. Chronis, J. Langerman, S. Fitz-Gibbon, L. Rubbi, R. J. P. Skelton, R. Ardehali, M. Pellegrini, W. E. Lowry, A. T. Clark, K. Plath, Human Embryonic Stem Cells Do Not Change Their X Inactivation Status during Differentiation. *Cell Reports* **18**, 54–67 (2017). doi:10.1016/j.celrep.2016.11.054 Medline
20. T. Nakamura, I. Okamoto, K. Sasaki, Y. Yabuta, C. Iwatani, H. Tsuchiya, Y. Seita, S. Nakamura, T. Yamamoto, M. Saitou, A developmental coordinate of pluripotency among mice, monkeys and humans. *Nature* **537**, 57–62 (2016). doi:10.1038/nature19096 Medline
21. H. Ohta, K. Kurimoto, I. Okamoto, T. Nakamura, Y. Yabuta, H. Miyauchi, T. Yamamoto, Y. Okuno, M. Hagiwara, K. Shirane, H. Sasaki, M. Saitou, *In vitro* expansion of mouse primordial germ cell-like cells recapitulates an epigenetic blank slate. *EMBO J.* **36**, 1888–1907 (2017). doi:10.15252/embj.201695862 Medline
22. H. Miyauchi, H. Ohta, S. Nagaoka, F. Nakaki, K. Sasaki, K. Hayashi, Y. Yabuta, T. Nakamura, T. Yamamoto, M. Saitou, Bone morphogenetic protein and retinoic acid synergistically specify female germ-cell fate in mice. *EMBO J.* **36**, 3100–3119 (2017). doi:10.15252/embj.201796875 Medline
23. T. Sakuma, S. Hosoi, K. Woltjen, K. Suzuki, K. Kashiwagi, H. Wada, H. Ochiai, T. Miyamoto, N. Kawai, Y. Sasakura, S. Matsuura, Y. Okada, A. Kawahara, S. Hayashi, T. Yamamoto, Efficient TALEN construction and evaluation methods for human cell and animal applications. *Genes Cells* **18**, 315–326 (2013). doi:10.1111/gtc.12037 Medline
24. J. Chaumeil, I. Okamoto, E. Heard, X-chromosome inactivation in mouse embryonic stem cells: Analysis of histone modifications and transcriptional activity using immunofluorescence and FISH. *Methods Enzymol.* **376**, 405–419 (2004). doi:10.1016/S0076-6879(03)76027-3 Medline
25. J. Chaumeil, S. Augui, J. C. Chow, E. Heard, Combined immunofluorescence, RNA fluorescent in situ hybridization, and DNA fluorescent in situ hybridization to study chromatin changes, transcriptional activity, nuclear organization, and X-chromosome inactivation. *Methods Mol. Biol.* **463**, 297–308 (2008). doi:10.1007/978-1-59745-406-3_18 Medline
26. T. Nakamura, Y. Yabuta, I. Okamoto, S. Aramaki, S. Yokobayashi, K. Kurimoto, K. Sekiguchi, M. Nakagawa, T. Yamamoto, M. Saitou, SC3-seq: A method for highly parallel and quantitative measurement of single-cell gene expression. *Nucleic Acids Res.* **43**, e60 (2015). doi:10.1093/nar/gkv134 Medline
27. H. Li, B. Handsaker, A. Wysoker, T. Fennell, J. Ruan, N. Homer, G. Marth, G. Abecasis, R. Durbin; 1000 Genome Project Data Processing Subgroup, The Sequence Alignment/Map format and SAMtools. *Bioinformatics* **25**, 2078–2079 (2009). doi:10.1093/bioinformatics/btp352 Medline
28. W. Huang, B. T. Sherman, R. A. Lempicki, Systematic and integrative analysis of large gene lists using DAVID bioinformatics resources. *Nat. Protoc.* **4**, 44–57 (2009). doi:10.1038/nprot.2008.211 Medline
29. F. Miura, Y. Enomoto, R. Dairiki, T. Ito, Amplification-free whole-genome bisulfite sequencing by post-bisulfite adaptor tagging. *Nucleic Acids Res.* **40**, e136 (2012). doi:10.1093/nar/gks454 Medline
30. K. Shirane, K. Kurimoto, Y. Yabuta, M. Yamaji, J. Satoh, S. Ito, A. Watanabe, K. Hayashi, M. Saitou, H. Sasaki, Global Landscape and Regulatory Principles of DNA Methylation Reprogramming for Germ Cell Specification by Mouse Pluripotent Stem Cells. *Dev. Cell* **39**, 87–103 (2016). doi:10.1016/j.devcel.2016.08.008 Medline
31. R. S. Illingworth, U. Gruenewald-Schneider, S. Webb, A. R. W. Kerr, K. D. James, D. J. Turner, C. Smith, D. J. Harrison, R. Andrews, A. P. Bird, Orphan CpG islands identify numerous conserved promoters in the mammalian genome. *PLOS Genet.* **6**, e1001134 (2010). doi:10.1371/journal.pgen.1001134 Medline
32. F. Court, C. Tayama, V. Romanelli, A. Martin-Trujillo, I. Iglesias-Platas, K. Okamura, N. Sugahara, C. Simón, H. Moore, J. V. Harness, H. Keirstead, J. V. Sanchez-Mut, E. Kaneki, P. Lapunzina, H. Soejima, N. Wake, M. Esteller, T. Ogata, K. Hata, K. Nakabayashi, D. Monk, Genome-wide parent-of-origin DNA methylation analysis reveals the intricacies of human imprinting and suggests a germline methylation-independent mechanism of establishment. *Genome Res.* **24**, 554–569 (2014). doi:10.1101/gr.164913.113 Medline
33. R. Lister, M. Pelizzola, R. H. Dowen, R. D. Hawkins, G. Hon, J. Tonti-Filippini, J. R. Nery, L. Lee, Z. Ye, Q.-M. Ngo, L. Edsall, J. Antosiewicz-Bourget, R. Stewart, V. Ruotti, A. H. Millar, J. A. Thomson, B. Ren, J. R. Ecker, Human DNA methylomes at base resolution show widespread epigenomic differences. *Nature* **462**, 315–322 (2009). doi:10.1038/nature08514 Medline
34. R. Lister, M. Pelizzola, Y. S. Kida, R. D. Hawkins, J. R. Nery, G. Hon, J. Antosiewicz-Bourget, R. O'Malley, R. Castanon, S. Klugman, M. Downes, R. Yu, R. Stewart, B. Ren, J. A. Thomson, R. M. Evans, J. R. Ecker, Hotspots of aberrant epigenomic reprogramming in human induced pluripotent stem cells. *Nature* **471**, 68–73 (2011). doi:10.1038/nature09798 Medline

ACKNOWLEDGMENTS

We thank the members of our laboratory for their helpful input on this study: K. Hayashi for his advice on rOvaries, and Y. Nagai, Y. Sakaguchi, and M. Kawasaki of the Saitou Laboratory, J. Oishi of the Sasaki Laboratory, and T. Sato and M. Kabata of the Yamamoto Laboratory for their technical assistance, and the Center for Anatomical, Pathological and Forensic Medical Research at Kyoto University for the preparation of electron microscopy. We also thank T. Mori for his encouragement and support. **Author contributions:** C.Y. performed hPGCLC induction, and xrOvary formation and analysis. K.S., Y.K. and S.Y. assisted in hPGCLC induction, and Y.I. assisted in xrOvary formation. T.N. and T.Y. contributed to the RNA-seq/WGBS, Y.M., K.S. and H.S. contributed to the WGBS, and Y.Y. contributed to the analyses of RNA-seq/WGBS data. I.O. performed the RNA FISH. Y.K. and M.S. designed the experiments and wrote the manuscript. **Funding:** This work was supported by a Grant-in-Aid for Specially Promoted Research from JSPS (17H06098) to M.S., by a JST-ERATO Grant (JPMJER1104) to M.S., and by a Grant-in-Aid for Scientific Research on Innovative Areas from JSPS to H.S. (25112010). **Competing interests:** The authors declare no competing interests. **Data and materials availability:** The accession numbers for the RNA-seq and WBGS data generated in this study are GSE117101 (GEO) and DRA006618/DRA007077 (DDBJ), respectively.

SUPPLEMENTARY MATERIALS

www.sciencemag.org/cgi/content/full/science.aat1674/DC1
Materials and Methods
Figs. S1 to S17
References (*23*–*34*)
Tables S1 to S6

1 February 2018; accepted 10 September 2018
Published online 20 September 2018
10.1126/science.aat1674

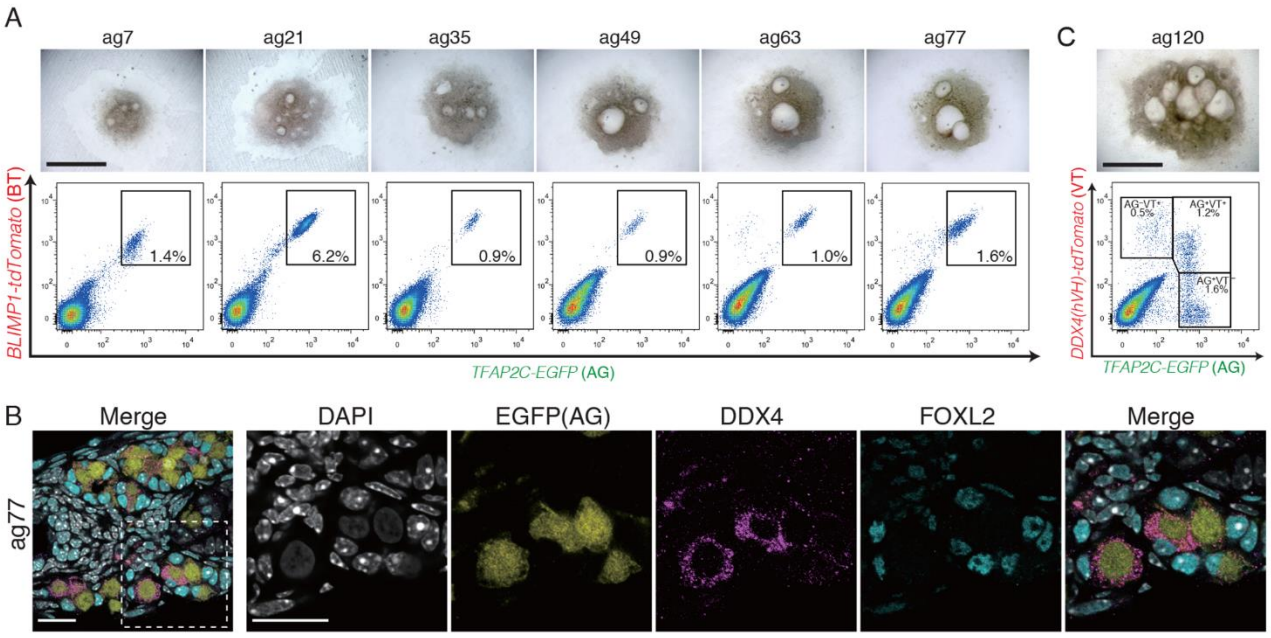

Fig. 1. hPGCLC differentiation in xrOvaries. (**A**) Bright field (BF) images and FACS by BTAG (*BLIMP1-tdTomato*; *TFAP2C-EGFP*) of xrOvaries with 585B1 BTAG (XY) hPGCLC-derived cells from ag7 to ag77. Bars in (A, C), 500 μm. (**B**) Expression of DDX4 (magenta) in AG$^+$ cells (yellow) in xrOvaries at ag77, with FOXL2 (cyan) and DAPI (white) staining. The boxed area in the left panel (merged image) is magnified in the right panels. Bars, 20 μm. (**C**) A BF image and FACS by AGVT (*DDX4/hVH-tdTomato*) of xrOvaries at ag120 with 1390G3 AGVT (XX) hPGCLC-derived cells.

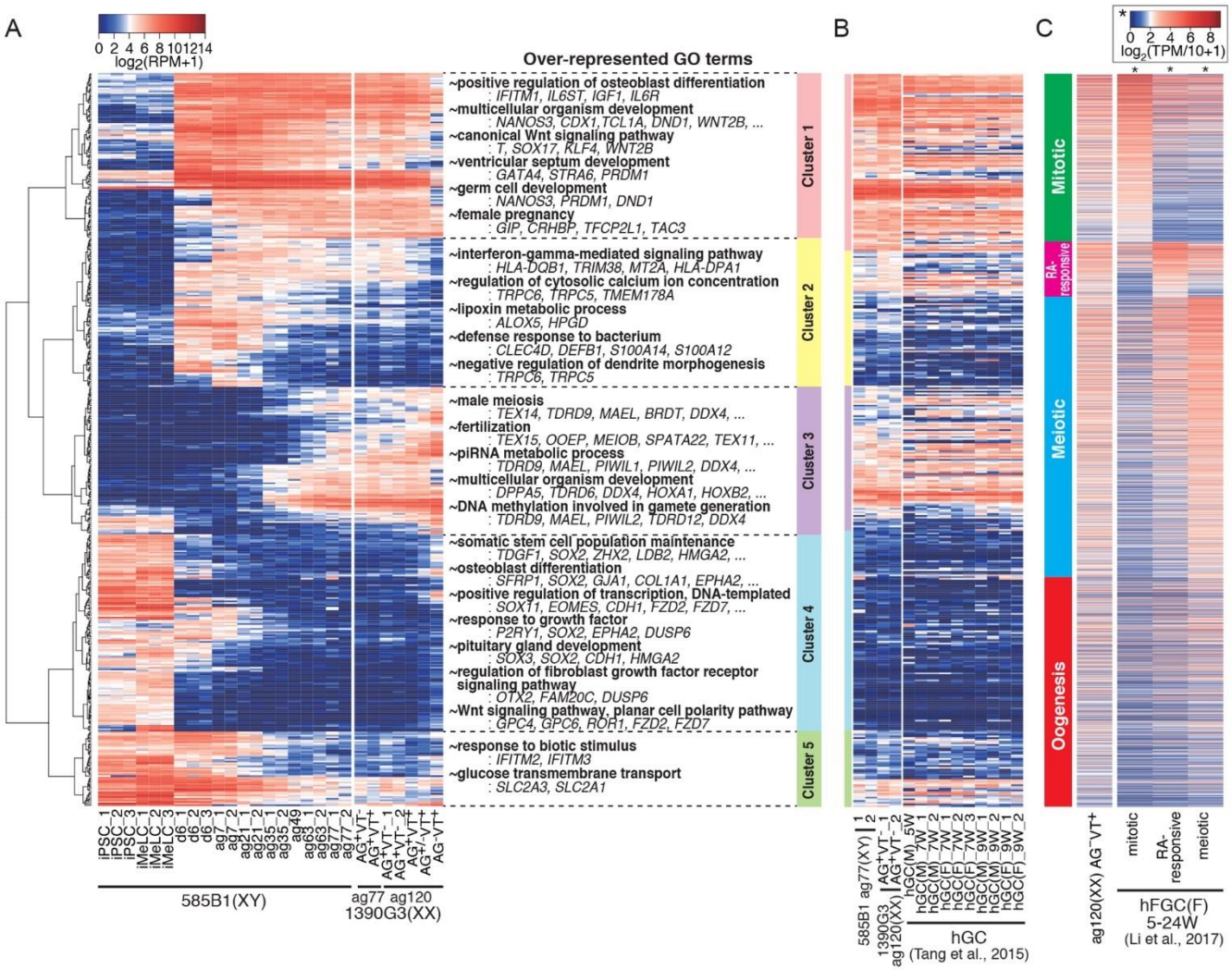

Fig. 2. Transcriptome dynamics of hPGCLC-derived cells in xrOvaries. (**A**) (left) Unsupervised hierarchical clustering (UHC) and heatmap of the expression in the indicated cells of the 453 signature genes for the transitions of hPGCLC-derived cell properties in xrOvaries (Fig. S8C, D, Table S2). (right) Representative genes in each cluster and their GO enrichments (Table S2). (**B** and **C**) Comparison of the expression of the 453 (B) or indicated genes (*14*) (C) between ag77 BT^+AG^+ and ag120 AG^+VT^+ cells (B) or ag120 AG^-VT^+ cells (C) and the indicated human germ cells (*12*, *14*).

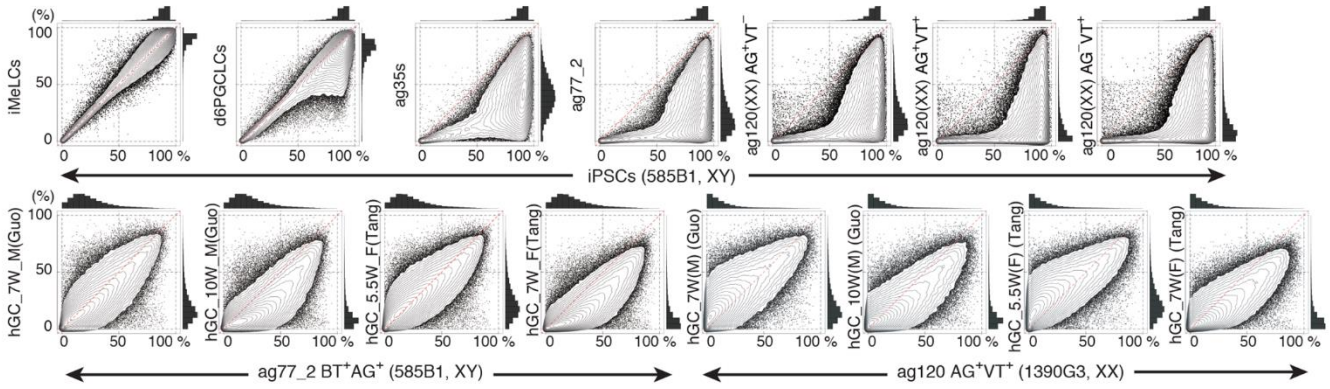

Fig. 3. Genome-wide DNA demethylation in hPGCLC-derived cells in xrOvaries. Comparisons of the 5mC levels (genome-wide 2-kb windows) by contour representations of scatter plots, combined with histogram representations (top and right of scatter plots), between hiPSCs (top) or ag77 BT^+AG^+ cells (bottom, left)/ag120 AG^+VT^+ cells (bottom, right) and the indicated cell types.

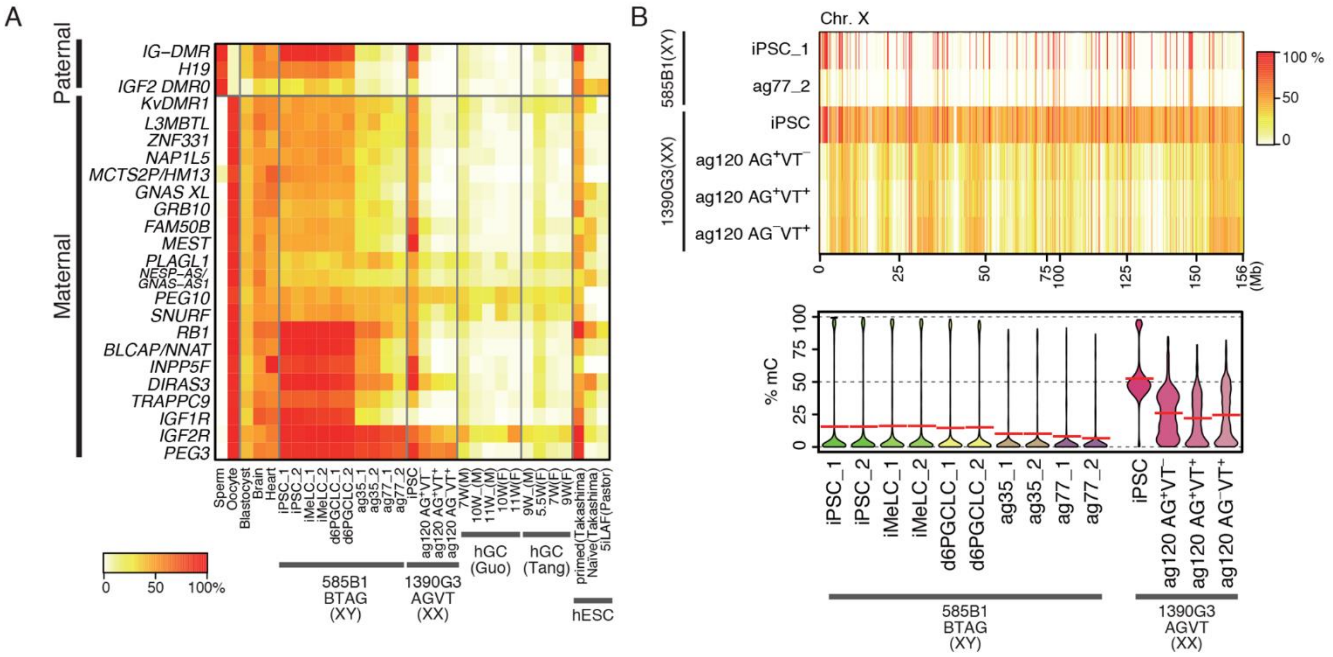

Fig. 4. Imprint erasure and X chromosome demethylation in hPGCLC-derived cells in xrOvaries. (**A**) Heatmaps showing the 5mC levels in the differentially methylated regions (DMRs) of the indicated imprinted genes in the indicated cells. (**B**) Heatmaps (top) and violin plots (bottom, average: red bars) showing the 5mC levels in the CpG islands on the X chromosomes in the indicated cells.

Generation of human oogonia from induced pluripotent stem cells in vitro

Chika Yamashiro, Kotaro Sasaki, Yukihiro Yabuta, Yoji Kojima, Tomonori Nakamura, Ikuhiro Okamoto, Shihori Yokobayashi, Yusuke Murase, Yukiko Ishikura, Kenjiro Shirane, Hiroyuki Sasaki, Takuya Yamamoto and Mitinori Saitou

published online September 20, 2018